Chaotic Hierarchy in a Model of Competing Populations

GEROLD BAIER[1], JESPER S. THOMSEN[2] AND ERIK MOSEKILDE[2]

[1] *Institute for Chemical Plant Physiology*
University of Tübingen
D-7400 Tübingen, FRG

[2] *System Dynamics Group*
Physics Laboratory III
Technical University of Denmark
DK-2800 Lyngby, Denmark

Running Headline: Higher Chaos in Competing Populations

Abstract

The dynamics of a deterministic model for the interaction of populations of bacteria attacked by phages is analyzed. We find that the basic system with one type of bacteria and phages can show oscillations in a CSTR. Two, three, and four competing populations show chaos, hyperchaos, and chaos with three positive Lyapunov exponents, respectively. We discuss the principle of generating complexity by coupling of oscillators with a common feeding source.

1 Introduction

Time series in population dynamics often show stochastic features. They resemble noise rather than explainable structure, and the deterministic basis for the dynamics has been a question of debate. A large number of empirical data have been analyzed with respect to the occurrence of chaos, and low-dimensional systems of ordinary differential equations have been proposed for the irregular ups and downs, e.g. in childhood epidemics (Olsen & Schaffer, 1990). In many cases, however, clear evidence for simple chaos could not be established and stochastic elements were introduced in the models to account for behavior where chaos failed to explain significant features (Olsen *et at.*, 1988). Clearly, different grades of irregularity are possible in the observed dynamics. It is of interest to investigate whether different grades of aperiodicity can be accounted for by deterministic models without explicitly introducing noise or random variables.

In an effort to bridge the gap between deterministic three-variable chaos and white noise with infinite degrees of freedom the idea of a chaotic hierarchy was introduced (Rössler, 1983). It was predicted that with increasing number of degrees of freedom the maximum complexity of a dynamical system could continue to increase. Starting from a closed periodic trajectory as an attracting solution, the action of stretching and folding in phase space can introduce divergence of nearby trajectories on a bounded attractor and result in stable chaotic behavior. However the procedure of stretching and folding, i.e. mixing, can be applied in more than one independent directions. In particular, systems with N deterministic variables ($N > 3$) may produce hyperchaotic behavior with up to $N - 2$ positive Lyapunov characteristic exponents (LCEs). In this work we investigate the occurrence of hyperchaos (Rössler, 1979; Thomsen *et al.*, 1992; Baier & Klein, 1990). in a model of bacteria-phage interaction. A main purpose is to illustrate a type of coupling between pray-predator systems which can produce thise complex forms of behavior.

2 The model

The model is given by the following set of ordinary differential equations for n populations of bacteria and their respective phages in a continuous flow stirred tank

reactor (CSTR) (Nielssen *et al.*, 1991)

$$\frac{dB_i}{dt} = \nu \frac{S\,B_i}{\kappa + S} - B_i(\rho + \alpha\,\omega P_i) \tag{1}$$

$$\frac{dI_{i1}}{dt} = \alpha\,\omega\,B_i P_i - \rho\,I_{i1} - \frac{3}{\tau}\,I_{i1} \tag{2}$$

$$\frac{dI_{i2}}{dt} = \frac{3}{\tau}\,(I_{i1} - I_{i2}) - \rho\,I_{i2} \tag{3}$$

$$\frac{dI_{i3}}{dt} = \frac{3}{\tau}\,(I_{i2} - I_{i3}) - \rho\,I_{i3} \tag{4}$$

$$\frac{dP_i}{dt} = \phi - P_i \sum_j \alpha\,B_j - \rho\,P_i + \frac{3}{\tau}\,\beta\,I_{i3} - P_i \sum_j \sum_k \alpha\,I_{jk} \tag{5}$$

$$\frac{dS}{dt} = \rho(\sigma - S) - \sum_j \gamma\nu \frac{S\,B_j}{\kappa + S} \tag{6}$$

These are the basic contributions to the model: Bacteria B feed autocatalytically on substrate S which is being fed continuously. The growth rate is described by a saturation function. Bacteria of type i are attacked by phages P_i to yield infected bacteria I_i. These are modelled using three delay variables I_{i1}, I_{i2}, and I_{i3}. Infected bacteria are destroyed after some delay time and release new phages. Phages can also adsorb to the walls of infected or noninfected bacteria. Parameters ν, κ, α, and ω describe, respectively, the bacterial growth rate with no resource constraints, the substrate concentration below which the bacterial growth rate decreases, the adsorption rate of phages on bacterial surfaces, and the infection probability. τ is the characteristic infectious period during which phages multiply in the bacterial cell. ϕ is an external supply of phages (the infection source). β is the bust size, i.e. the number of phages released in average by each infected bacterial cell. σ is the external supply of resources, and γ is the resource consumption per cell division.

Realistic parameters are given in Nielssen *et al.* (1991) to be: $\alpha = 10^{-9}$ l/min, $\omega = 0.8$, $\kappa = 10^4$ mg/l, $\nu = 0.024$ min^{-1}, $\gamma = 0.01$ mg, $\tau = 30$ min, $\beta = 100$, $\sigma = 10^4$ mg/l, and $\phi = 0.1$ l$^{-1}\cdot$min^{-1}.

Different from the original model designed for application in the dairy industry we have omitted cross-infection of bacteria B_i by phages P_j (i.e. off-diagonal elements in the ω matrix in Nielssen *et al.* (1991) are equal to zero). All other terms and parameters are kept as in Nielssen *et al.* (1991). We vary the dilution rate ρ and study the asymptotic dynamics of the equations. Reintroducing the cross-coupling

has been found not to alter the dynamics significantly.

3 Results

3.1 One population

In the simplest case only one population of bacteria and phages is considered. Bacteria feed on substrate and multiply. At the same time their number is decreased by successful attacks by phages. Phages multiply as a function of lysed infected bacteria. For large values of the dilution parameter ρ ($\rho > 0.0058$ min^{-1}) both bacteria and phages arrive at a stable steady state. The bacterial population successfully maintains a high level of individuals due to plenty of substrate. Fast dilution keeps the number of vira at a comparatively low level. The ratio of bacteria to phages is stable with respect to fluctuations. As ρ is decreased, however, the sensitivity to fluctuations grows and at $\rho = 0.0058$ min^{-1} the steady state looses stability. We find a Hopf bifurcation of a focus and for $\rho < 0.0058$ min^{-1} there are stable limit cycle oscillations with increasing amplitude as ρ is decreased further. The limit cycle is characterized by bursts in the phage population which drastically diminish the bacterium population. This in turn reduces the rate of viral replication. As vira are diluted and new substrate enters the flow reactor, bacteria recover and the cycle starts anew. For $\rho = 0$ the bacterium population dies out after some transient time depending on the chosen initial conditions. Numerically we did not find hysteresis or bistability in the bifurcation diagram. The single population bacterium-phage system is a dissipative Hopf oscillator with a supercritical transition.

3.2 Two populations

Next we consider a system with two identical bacterial populations each being subject to attack by a specific phage. As noted above only attacks of phage P_i on bacterium B_i are successful. Adsorption of phage P_i on bacterium B_j diminishes the number of phages but does not produce any infected bacteria. The two populations are treated the same except for initial conditions. In the bifurcation diagram Fig. 1, Poincaré cross-sections for $B_1 = B_2$ are displayed as a function of the dilution rate ρ. Starting at $\rho = 0.0050$ min^{-1} the system exhibits limit cycle oscillations with phase delay between the two populations. Decreasing ρ the limit cycle undergoes a

torus bifurcation to quasiperiodic solutions interrupted by phase locking as would be expected for the case of two coupled oscillators. The locked state of period seven shows period-doubling to a period 14 solution. Herafter the solution unlocks again and for still lower dilution rates the torus breaks down and becomes chaotic. Chaos is reached at $\rho \approx 0.00448$ min^{-1}, and the system stays chaotic as ρ is decreased further.

The chaotic range in parameter space seems to consist of two parts as judged from the structure of the bifurcation diagram. There is a change in the distribution of cross-section points at $\rho \approx 0.00402$ min^{-1}. To investigate this further we show another projection of the bifurcation diagram in Figs. 2a and 2b starting with two different initial conditions at high values of ρ. There are two chaotic attractors coexisting for $\rho > 0.00402$ min^{-1}. They merge to yield a single chaotic solution at $\rho \approx 0.00402$ min^{-1} and, judging from numerical treatment, the system appears to possess only one stable chaotic attractor for $\rho < 0.00402$ min^{-1}. Figs. 3a and 3b show cross-sections of the two coexisting chaotic attractors for two sets of initial conditions. They are both characteristic of fractalized two-tori and can indeed be shown to originate in two coexisting two-frequency quasiperiodic solutions. The transition in the structure of the chaotic solutions can now be attributed to a crisis associated with a collision of the coexisting chaotic attractors with their separating basin boundary. This boundary crisis (Grebogi *et al.*, 1987) is common in systems of two coupled oscillators. It is interesting to observe that the merged attractor conserves almost all features of the two coexisting attractors right before the crisis (Fig. 3c). We then arbitrarily chose a value for ρ in the chaotic region ($\rho = 0.0015$ min^{-1}) and calculated the spectrum of Lyapunov exponents for the corresponding attractor. We found: $\lambda_1 = 3.02 \cdot 10^{-4}$ min^{-1}, $\lambda_2 = 3.10 \cdot 10^{-6}$ min^{-1}, and $\lambda_3 = -2.06 \cdot 10^{-4}$ min^{-1}. The spectrum confirms chaos with one positive Lyapunov exponent. In addition $\lambda_1 + \lambda_3 > 0$, so the chaos is of the Kaplan-Yorke type (Kaplan & Yorke, 1979) with dimension larger than 3.

3.3 Three populations

In the same way as in the preceeding section we now extend the original oscillating unit to a system with three different populations feeding on continuously fed substrate in a CSTR. The system is herafter composed of 16 ordinary differential

equations. As might be expected the dynamic behavior is quite complicated so we describe the bifurcation diagram (Fig. 4) in some detail.

First we note that Fig. 4 has not been obtained for a single set of inital conditions followed adiabatically as ρ is decreased or increased. Several branches with sometimes coexisting solutions have been plotted on top of each other. For $\rho = 0.0065$ min^{-1} there are two coexisting period-one solutions both of which are found to stay stable down to $\rho \approx 0.0031$ min^{-1}. From $\rho \approx 0.00625$ min^{-1} to $\rho \approx 0.00600$ min^{-1} we find quasiperiodic motion and locked states on a folded two-torus. In the chosen cross-section ($B_1 = B_2$) the torus is cut twice by the Poincaré plane. Fig. 5 shows the attractor at $\rho = 0.00625$ min^{-1}. The largest Lyapunov exponents are found to be $4.24 \cdot 10^{-9}$ min^{-1}, $3.12 \cdot 10^{-9}$ min^{-1}, and $-1.24 \cdot 10^{-4}$ min^{-1} indicating quasiperiodicity. On both branches the system evolves antimonotonously (Dawson *et al.*, 1992) and there are several lockings of high periodicity as ρ is decreased followed by a transition to chaos via torus break-up. The chaotic attractor shown in Fig. 6 consists of small line segments, many of which show a typical folded shape. For the corresponding aperiodic time series the largest Lyapunov exponents are $4.3 \cdot 10^{-6}$ min^{-1}, $7.5 \cdot 10^{-8}$ min^{-1}, and $-1.9 \cdot 10^{-5}$ min^{-1} (a single positive exponent) and $\lambda_1 + \lambda_3 < 0$, thus there is simple chaos with a fractal dimension of the attractor $2 < D_F < 3$. The Lyapunov dimension was calculated to be $D_L = 2.23$.

The window in parameter space for simple chaos is small, however. At $\rho = 0.0055$ min^{-1} we find an attractor with different structure. The former islands are now connected and the shape resembles a closed but multiply twisted ribbon (Fig. 7). Calculating the LCE spectrum yields $\lambda_1 = 1.86 \cdot 10^{-5}$ min^{-1}, and $\lambda_3 = -1.49 \cdot 10^{-5}$ min^{-1}. Thus $\lambda_1 + \lambda_3 > 0$, and there is a jump in the integer part of the dimension of the chaotic attractor ($3 < D_F < 4$). The Lyapunov dimension formula gives $D_L = 3.01$.

As ρ is decreased toward $\rho \approx 0.0047$ min^{-1}, the width of the ribbon widens and the attractor becomes more and more sheet-like. At $\rho \approx 0.0047$ min^{-1} there is a crisis and the chaotic attractor disappears. Depending on initial conditions the system settles down to one of two coexisting period-one limit cycles. Period-one oscillations seem to be the only stable solutions as ρ is decreased until, for $\rho < 0.0037$ min^{-1}, aperiodic behavior is encountered again, this time coexisting with the period-one limit cycle down to $\rho \approx 0.0031$ min^{-1}. The cross-section of

the chaotic attractor at $\rho = 0.0035$ min^{-1} is plotted in Fig. 8. The structure is sheet-like, and the sheet obviously possesses foldings. The four largest LCEs are $\lambda_1 = 3.03 \cdot 10^{-4}$ min^{-1}, $\lambda_2 = 1.85 \cdot 10^{-4}$ min^{-1}, $\lambda_3 = -5.51 \cdot 10^{-8}$ min^{-1}, and $\lambda_4 = -3.41 \cdot 10^{-4}$ min^{-1}, confirming that the attractor produces hyperchaos (C^2) with two directions of stretching and folding. With $\lambda_1 + \lambda_4 > 0$ the Lyapunov dimension is $D_L = 4.16$. For $\rho < 0.0032$ min^{-1} the hyperchaotic attractor appears to be the only stable solution in our model for three populations.

3.4 Four populations

As a final numerical experiment we couple *four* populations of bacteria with their respective phages in the same way as before. The system starts with simple periodic oscillations for high values of ρ, and the complexity of the dynamics increases as ρ is decreased. As in the case of three coupled populations there are multiple coexisting solutions and phase space structure becomes complicated. Several types of chaos can be distinguished. Given the above results we expect the most complex type of behavior to dominate the system for small values of ρ. We arbitrarily chose $\rho = 0.0030$ min^{-1} and found chaos with a Poincaré cross-section that resembles a distorted cube in some projections. The basic difference when compared to simple hyperchaos is that a cross-section of in this regime of the four population model can no longer be adaquately embedded in three dimensions (Fig. 9). The six largest Lyapunov exponents are $\lambda_1 = 4.2 \cdot 10^{-4}$ min^{-1}, $\lambda_2 = 3.1 \cdot 10^{-4}$ min^{-1}, $\lambda_3 = 1.5 \cdot 10^{-4}$ min^{-1}, $\lambda_4 = 4.9 \cdot 10^{-7}$ min^{-1}, $\lambda_5 = -2.2 \cdot 10^{-4}$ min^{-1}, and $\lambda_6 = -6.7 \cdot 10^{-4}$ min^{-1}. There are three positive LCEs, i.e. hyper^2-chaos (C^3) with the convention used in Klein & Baier (1991). Applying the Kaplan-Yorke estimation for the Lyapunov dimension yields $D_L \approx 5.99$. This behavior is stable with respect to small changes in initial conditions as well as in ρ. Also, for $\rho < 0.0030$ min^{-1} the basin of this hyper^2-chaotic dynamics appears to dominate the phase space.

4 Discussion

In population dynamics it is often assumed that an ecological system tends to become more and more stable as additional species are introduced. Our work shows that this may not be the case, but that the complexity can continue to increase with

the number of species. Moreover, this complexity is found to be generic and to exist for a variety of different formulations of the interspecies interactions and for a wide range of parameter space, including parameter values which appear realistic for microbiological systems.

The system in eqs. (1–6) is a set of ordinary differential equations describing the interaction of bacteria and phages in a reduced and deterministic way. Arbitrary numbers of populations may be chosen. The one population oscillator consists of two coupled amplification rules. First, B grows autocatalytically on expense of S. Second, P grows in a loop that is fed on B. In principle, this set of differential equations could as well describe a chemical reaction scheme.

The numerical simulation of more than one population reveals the following general features. In all cases studied there is a unique solution for "high" values of ρ, as well as for "low" values of ρ. For high values there is a stable steady state of both bacteria and phages, and the steady state is homogeneous, i.e. same values for identical populations. No symmetry breaking is observed for high ρ. For low values the system exhibited the most complex type of behavior in scans of parameter ρ. This behavior was chaotic and included all populations likewise in the three cases studied. There are no obvious differences in the statistics of the variables for different populations. The bifurcation diagrams from high to low values of ρ show increasing complexity as the number of populations is increased. Particularly we find that due to the symmetry of the systems with more than one population multiple coexisting solutions appear. For the three population system some preliminary evidence for fractal basin boundaries between coexisting attractors was found (Nielssen *et al.*, 1991).

Here we wish to focus on the dynamics of the most complex attractor for low values of ρ. The systems with one, two, three, and four populations possess zero, one, two, and three positive Lyapunov exponents, respectively, in the most complex case. It appears that each time a population is added the maximum number of positive LCEs increases by one. Even though it might be assumed naively that coupling of increasing number of nonlinear subsystems may lead to the possibility of more complex dynamics in phase space it is a common experience that, for instance, diffusive coupling of nonlinear oscillators does not in general lead to hyperchaotic solutions (Kennedy & Aris, 1980). In our case, in contrast, it was not even necessary

to adjust more than one parameter to safely find chaos with three positive LCEs in the four population model.

We suggest that it is the particular type of coupling that allows one to create hyperchaotic solutions. The one population subsystem settles to a stable steady state for high values of ρ, i.e., for conditions with sufficient supply of substrate and efficient wash-out of phages. As supply of substrate and flow through the reactor are decreased the steady state looses stability and creates oscillatory dynamics. If more than one population is present then the same holds true for each subsystem. In addition, populations compete for a constant supply of the same source of food. This competition for one common substrate causes the suboscillations to interfere with each other creating ever higher chaotic trajectories as more of the oscillating subsystems are coupled.

In the case of diffusively coupled chaotic attractors a transition from homogeneous chaotic solution to hyperchaos via locked states has been demonstrated for decreasing coupling strength (Badola *et al.*, 1991). In contrast, in our system no driving system which itself is chaotic is required and coupling between substrate and bacteria is left unchanged. Substrate-coupled oscillators generate toroidal behavior and chaos arises from distortion of the torus. In the two-population model with simple chaos the Lyapunov dimension exceeds three but the third Lyapunov exponent stays negative and never reaches zero. Only one direction of stretching and folding takes place, resulting in a fat fractal torus. In the three population system we also observe this type of chaos (Fig. 7) but this time, as ρ is decreased, the largest of the negative exponents reaches zero and leads to a second positive one. On the torus, stretching and folding occurs in a second independent direction. Similarly, in the four population model a third direction of divergence in phase space occurs. Our system thus is a first candidate for an explicit model realizing the hierarchy of chaotic events under realistic assumptions (Rössler, 1983).

For further investigation of this principle we have simplified the system of eqs. (1–6) by omitting the two linear delay equations for I_{i2} and I_{i3} (coupling I_{i1} instead of I_{i3} to the phage variable P). Also we put $\omega = 1$ and omitted *all* cross-couplings between populations (adsorption of phage i to bacteria and infected bacteria j, $i \neq j$. We end up with a system of identical populations, each population consisting of three equations which are isolated except for the sole fact that they feed on

the same substrate. Performing simulations with all other constants as before we find that again for low values of ρ the new systems with one, two, three, and four populations produce attractors with zero, one, two, and three positive Lyapunov exponents. This confirms that coupling of identical subsystems to one common substrate is the source for higher chaos in our system.

The model may help explain observed variations in the size of competing populations on deterministic grounds and offer one appraoch to the understanding of hyperchaotic time series gained from experiments (like, for example, in space-time catalysis (Kruel *et al.*, 1992)). In the case of competing populations in a CSTR in the dairy industry higher chaos might be an event to avoid. A steady state with stable (reliable) quantities of each variant of bacteria is likely to be more welcome than hard to predict hyperchaotic oscillations. If, on the other hand, higher chaos occurs in a natural surrounding of competing populations then deterministic interaction leads to higher degrees of variability and to more effective mixing of configurations. It is an open question whether, in an evolutionary context, complex dynamics can be of any advantage for the system as a whole and thus turn competition of single species into cooperativity on a higher level. And finally, if, in chemical and biochemical reaction systems, higher chaos proves to play a role as (abstract) information generator then the proposed principle suggests one way how coupled units might reach maximum dynamical complexity.

G.B. thanks the Technical University of Denmark for generous support during his stay in Lyngby.

REFERENCES

BADOLA, P., KUMAR, V.R. & KULKARNI, B.D. (1991). Phys. Lett. A **155**, 365-372.

BAIER, G. & KLEIN, M. (1990). Phys. Lett. A **151**, 281-284.

DAWSON, S.P., GREBOGI, C., YORKE, J.A., KAN, I. & KOCAK, H. (1992). Phys. Lett. A **162**, 249-254.

GREBOGI, C., OTT, E. & YORKE, J.A. (1987). Physica **24D**, 243-262.

KAPLAN, J.L. & YORKE, J.A. (1979). In: Functional Differential Equations and Fixed Points. Lecture Notes in Mathematics 730 (Peitgen, H-O. & Walther, H-O. eds) p. 204-227. Berlin: Springer.

KENNEDY, C.R. & ARIS, R. (1980). In: New Approaches to Nonlinear Problems in Dynamics (Holmes, P.-J., ed) p. 211-233. Philadelphia SIAM.

KLEIN, M. & BAIER, G. (1991). In: A Chaotic Hierarchy (Baier, G. & Klein, M., eds) p. 1-23. Singapore: World Scientific.

KRUEL, TH.-M., SCHNEIDER, F.W., EISWIRTH, M. & ERTL, G. (1992). Chem. Phys. Lett. **193**, 305-310.

NIELSSEN, A.B., STRANDDORF, H.C.K. & MOSEKILDE, E. (1991). In: Proceedings of the 1991 European Simulation Multiconference, p. 751-756. San Diego: Simulation Councils Inc.

OLSEN, L.F. & SCHAFFER, W.M. (1990). Science **249**, 499-504.

OLSEN, L.F., TRUTY, G.L. & SCHAFFER, W.M. (1988). Theoret. Popul. Biol. **33**, 344-349.

RÖSSLER, O.E. (1979). Phys. Lett. A **71**, 155-157.

RÖSSLER, O.E. (1983). Z. Naturforsch. **38a**, 788-801.

THOMSEN, J.S., MOSEKILDE, E. & STERMAN, J.D. (1992). J. Systems Analysis and Modelling Simulation, **9**, 137-156.

Figure Captions

Fig. 1: Bifurcation diagram for system with two populations of bacteria. Started with initial conditions: $(S)_0 = 0.0, (B_1)_0 = 25000\ \mathrm{l}^{-1}, (B_2)_0 = 25118\ \mathrm{l}^{-1}$, all other initial conditions equal to zero, at $\rho = 0.0050\ \mathrm{min}^{-1}$ and followed adiabatically with a step size of $\Delta\rho = 2.0 \cdot 10^{-6}\ \mathrm{min}^{-1}$. For each value of ρ a transient trajectory of 10^5 min was omitted, and some cross-sections taken at $B_1 = B_2$ were plotted. Numerical integration was performed using custom made 5-6 order Runge-Kutta integration method with variable time step and error control.

Fig. 2: Detail of bifurcation diagram for two population model near $\rho = 0.0040\ \mathrm{min}^{-1}$. For cross-sections taken at $B_1 = B_2$ variable I_{i1} is plotted starting with initial conditions: a) $(S)_0 = 10.0\ \mathrm{mg/l}, (B_1)_0 = 20000\ \mathrm{l}^{-1}, (B_2)_0 = 10000\ \mathrm{l}^{-1}$. all other initial conditions equal to zero; and b) $(S)_0 = 0.0, (B_1)_0 = 25000\ \mathrm{l}^{-1}, (B_2)_0 = 25118\ \mathrm{l}^{-1}$,

Fig. 3: Chaotic attractors in the two population model in the neighborhood of a crisis. a) $\rho = 0.00404\ \mathrm{min}^{-1}, (S)_0 = 10.0\ \mathrm{mg/l}, (B_1)_0 = 20000\ \mathrm{l}^{-1}, (B_2)_0 = 10000\ \mathrm{l}^{-1}$; and b) $\rho = 0.00404\ \mathrm{min}^{-1}, (S)_0 = 0.0, (B_1)_0 = 25000\ \mathrm{l}^{-1}, (B_2)_0 = 25118\ \mathrm{l}^{-1}$; c) $\rho = 0.00401\ \mathrm{min}^{-1}$, initial conditions as in 4b. Attractors in a) and b) are coexisting, attractor in c) combines features of former coexisting attractors.

Fig. 4: Bifurcation diagram of three population model. Several coexisting solutions are plotted, made from adiabatic scans with both increasing and decreasing ρ. For $0.0\ \mathrm{min}^{-1} < \rho < 0.0030\ \mathrm{min}^{-1}$ only hyperchaos was found.

Fig. 5: Quasiperiodic attractor in the three population model. $\rho = 0.00625\ \mathrm{min}^{-1}$, cross-section taken at $B_1 = B_2$.

Fig. 6: Simple chaotic attractor in the three population model. $\rho = 0.005505\ \mathrm{min}^{-1}$, cross-section taken at $B_1 = B_2$.

Fig. 7: "Kaplan-Yorke" chaotic attractor in the three population model. $\rho = 0.00550\ \mathrm{min}^{-1}$, cross-section taken at $B_1 = B_2$.

Fig. 8: Hyperchaotic attractor in the three population model. $\rho = 0.0035$ min^{-1}, cross-section taken at $B_1 = B_2$.

Fig. 9: Hyper^2-chaotic attractor in the four population model. $\rho = 0.0030$ min^{-1}, cross-section taken at $B_1 = B_2$.

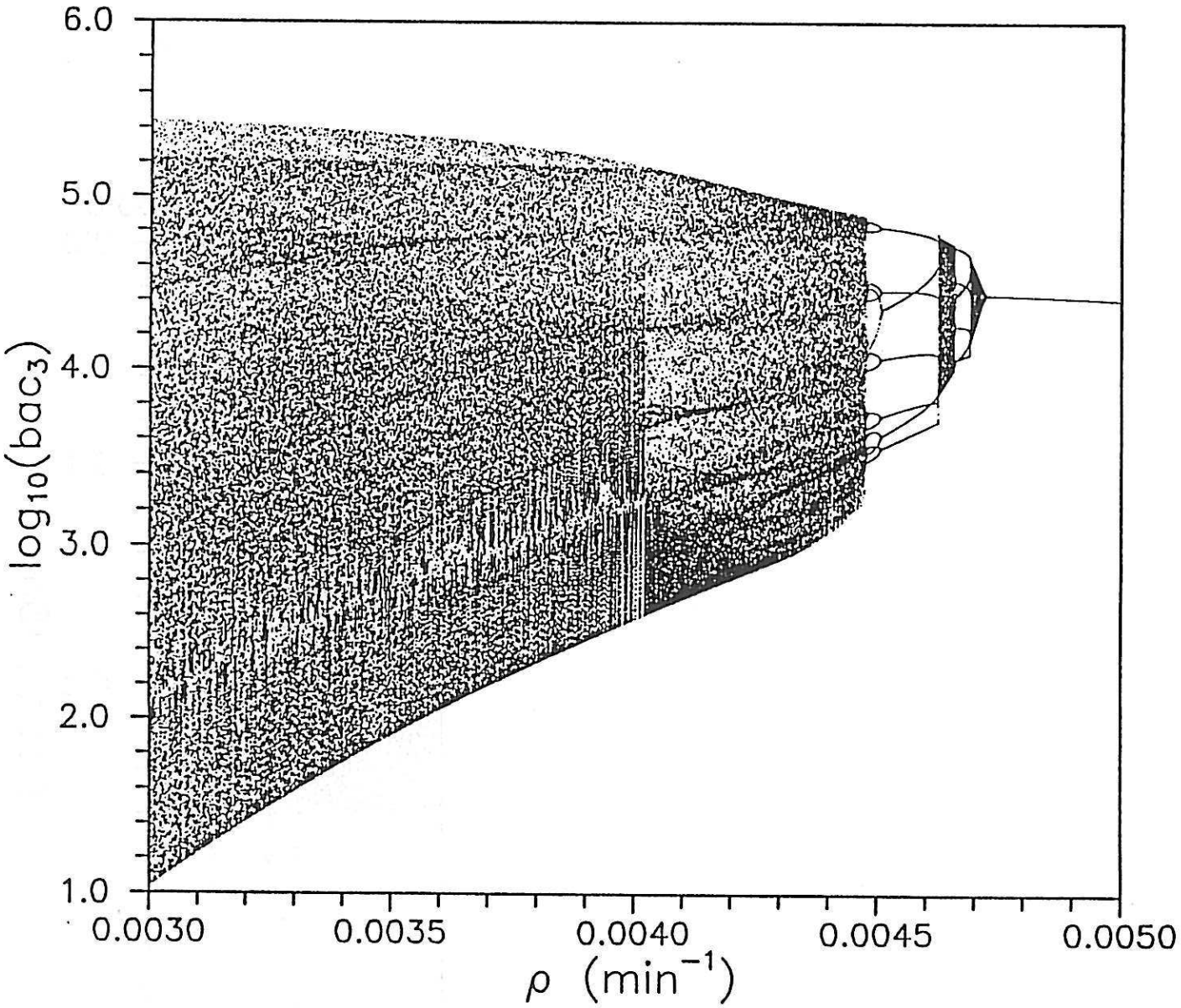

Baier et al.
Fig. 1

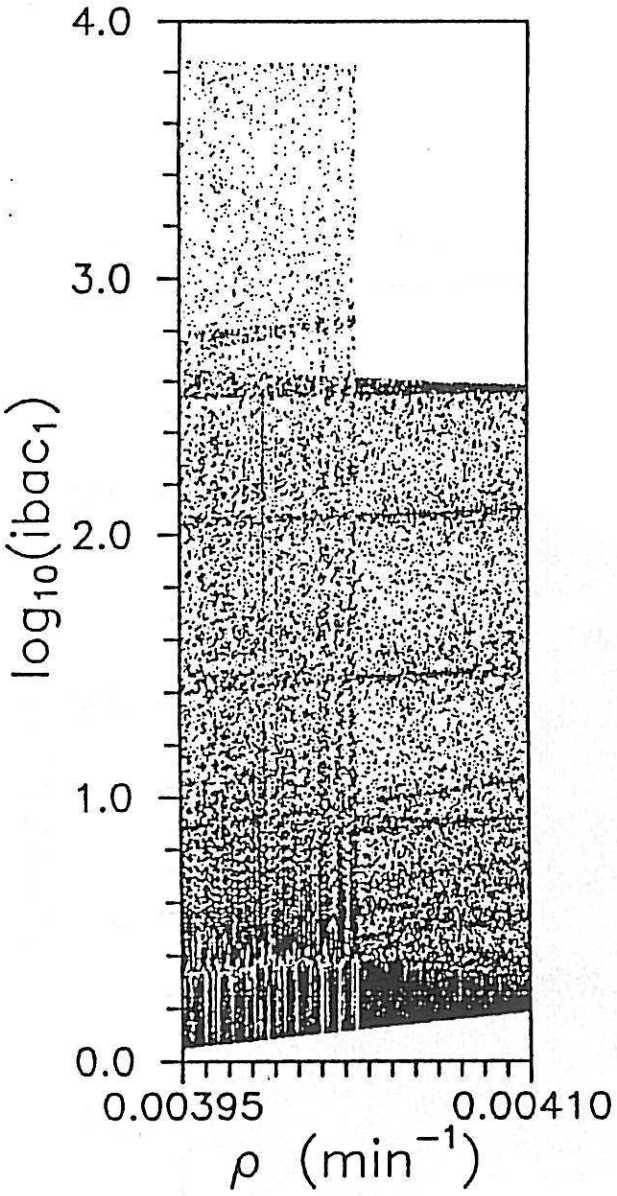

a

Baier et al.
Fig. 2a

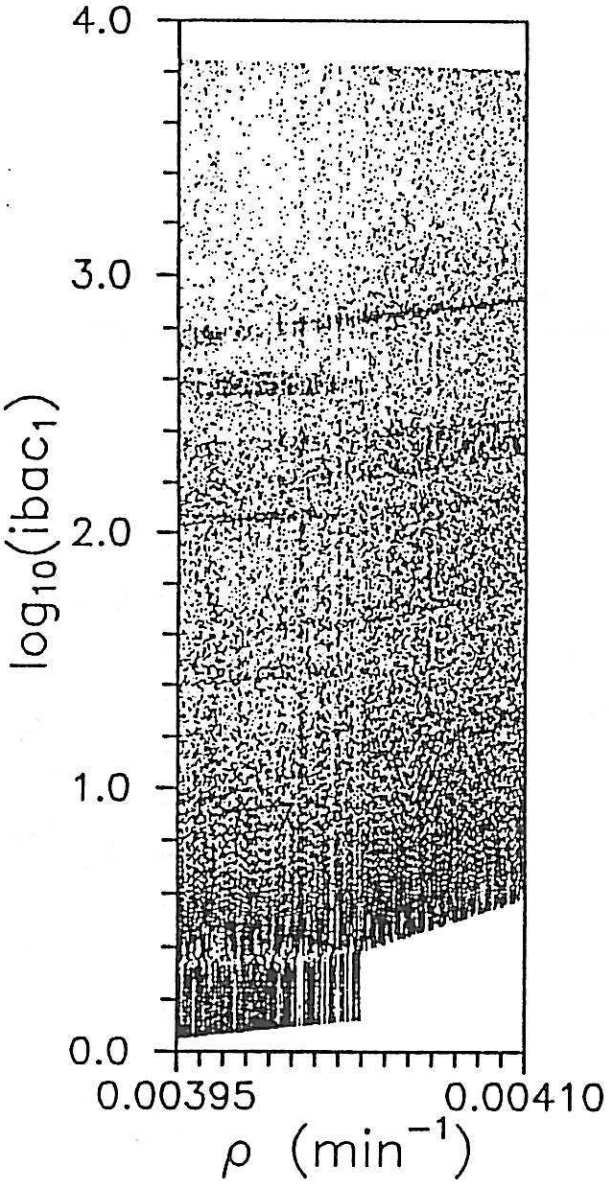

b

Baier et al.
Fig. 2b

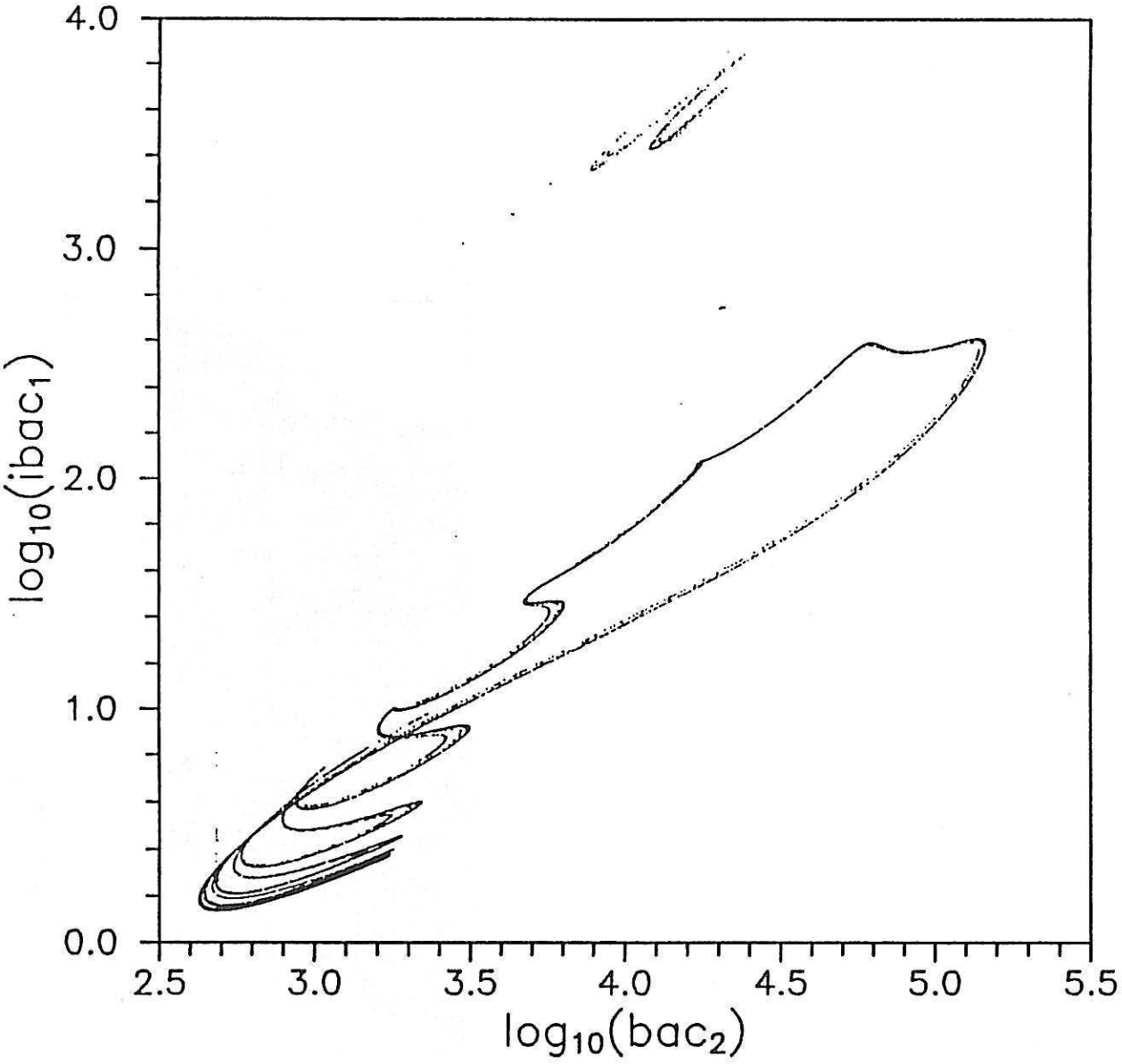

a

Baier et al.
Fig. 3a

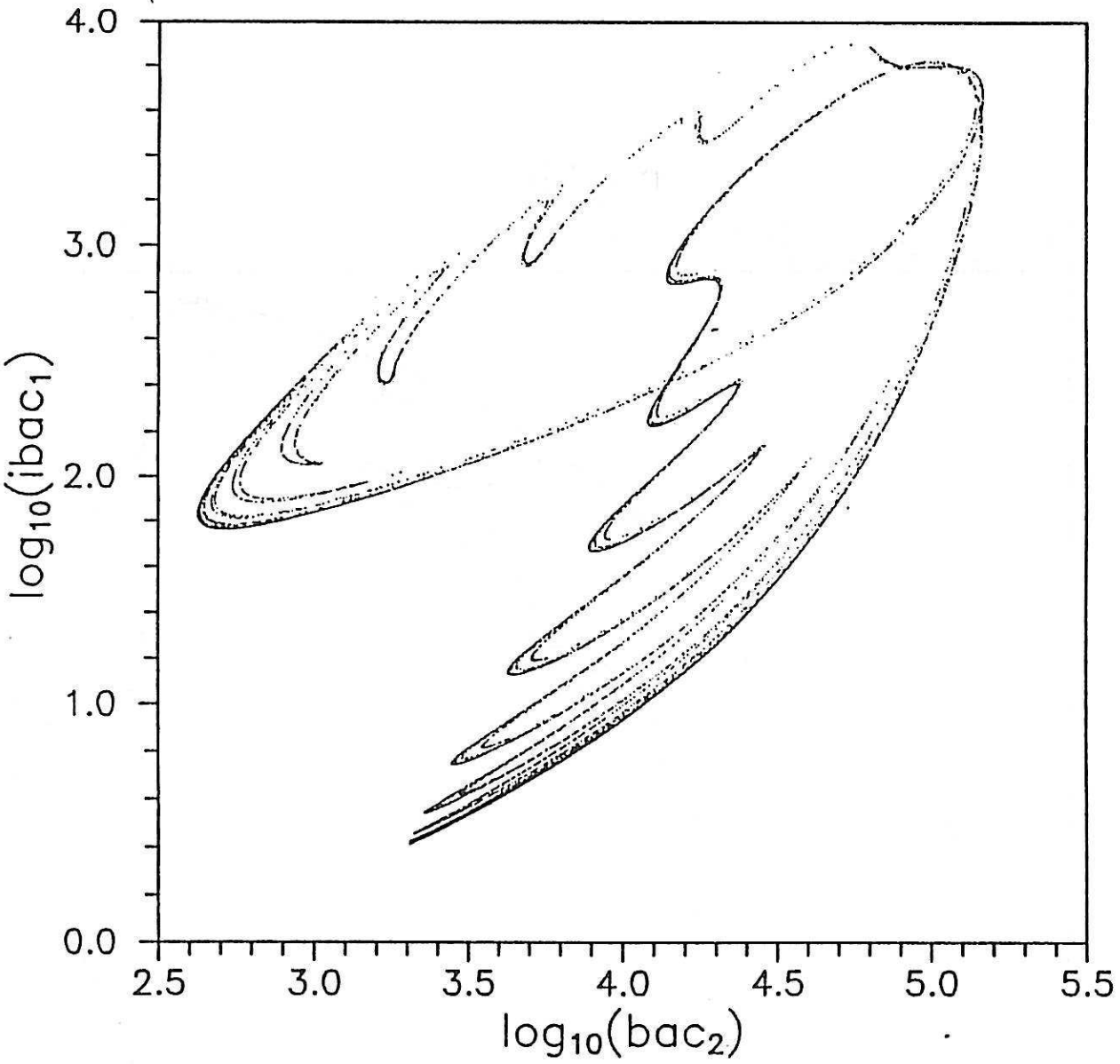

b

Baier et al.
Fig. 3b

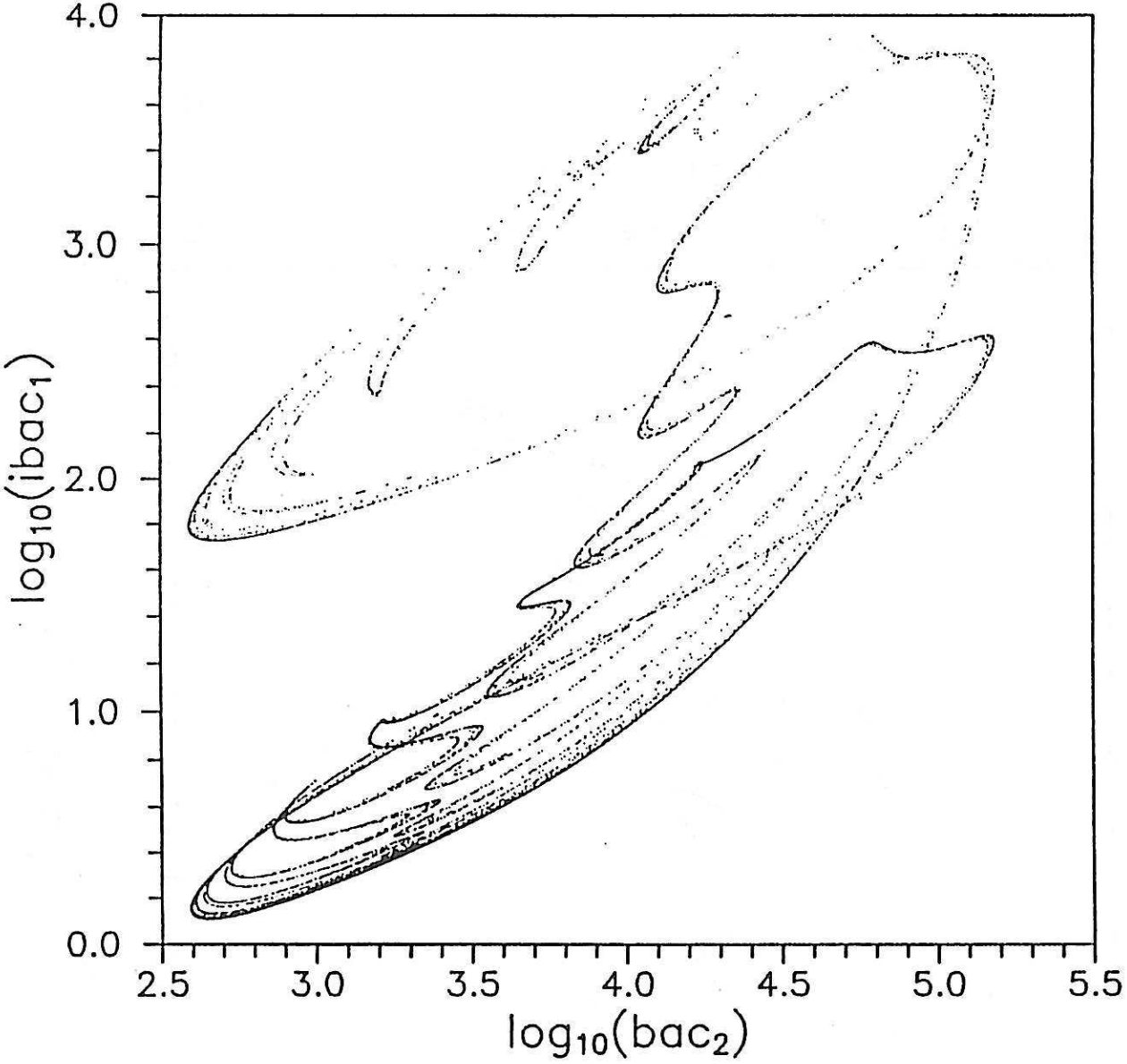

c

Baier et al.
Fig. 3c

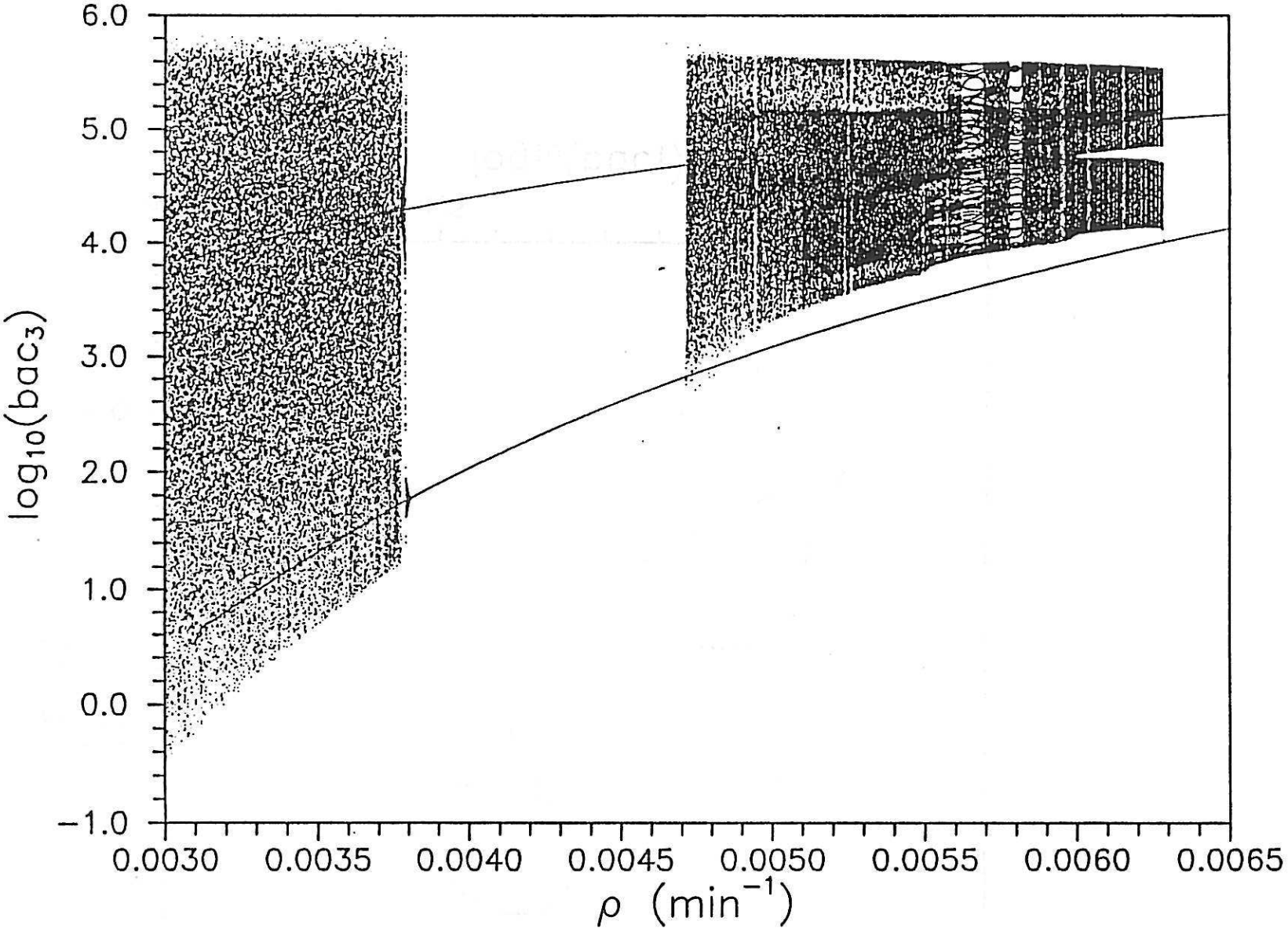

Baier et al.
Fig. 4

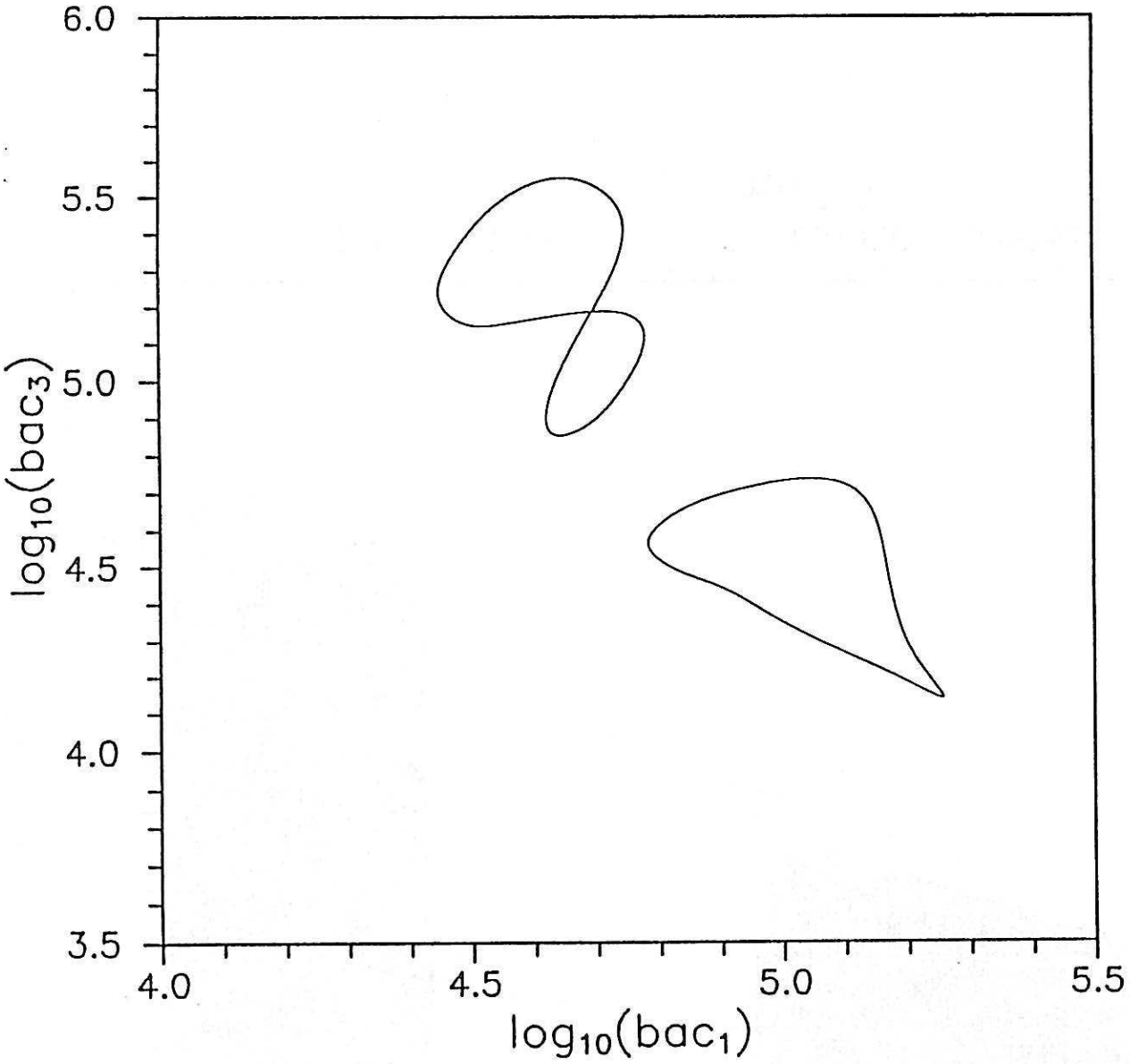

Baier et al.
Fig. 5

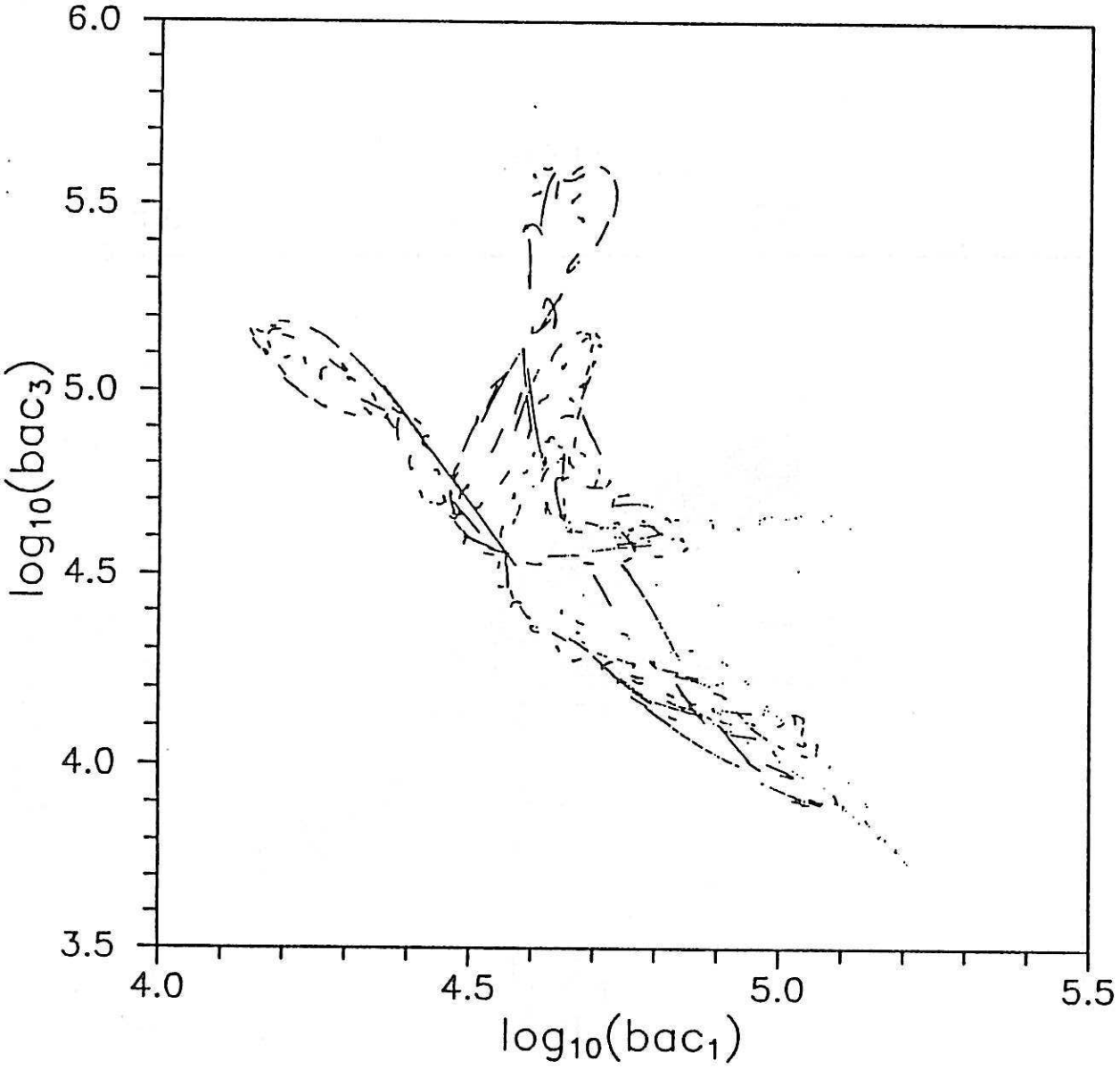

Baier et al.
Fig. 6

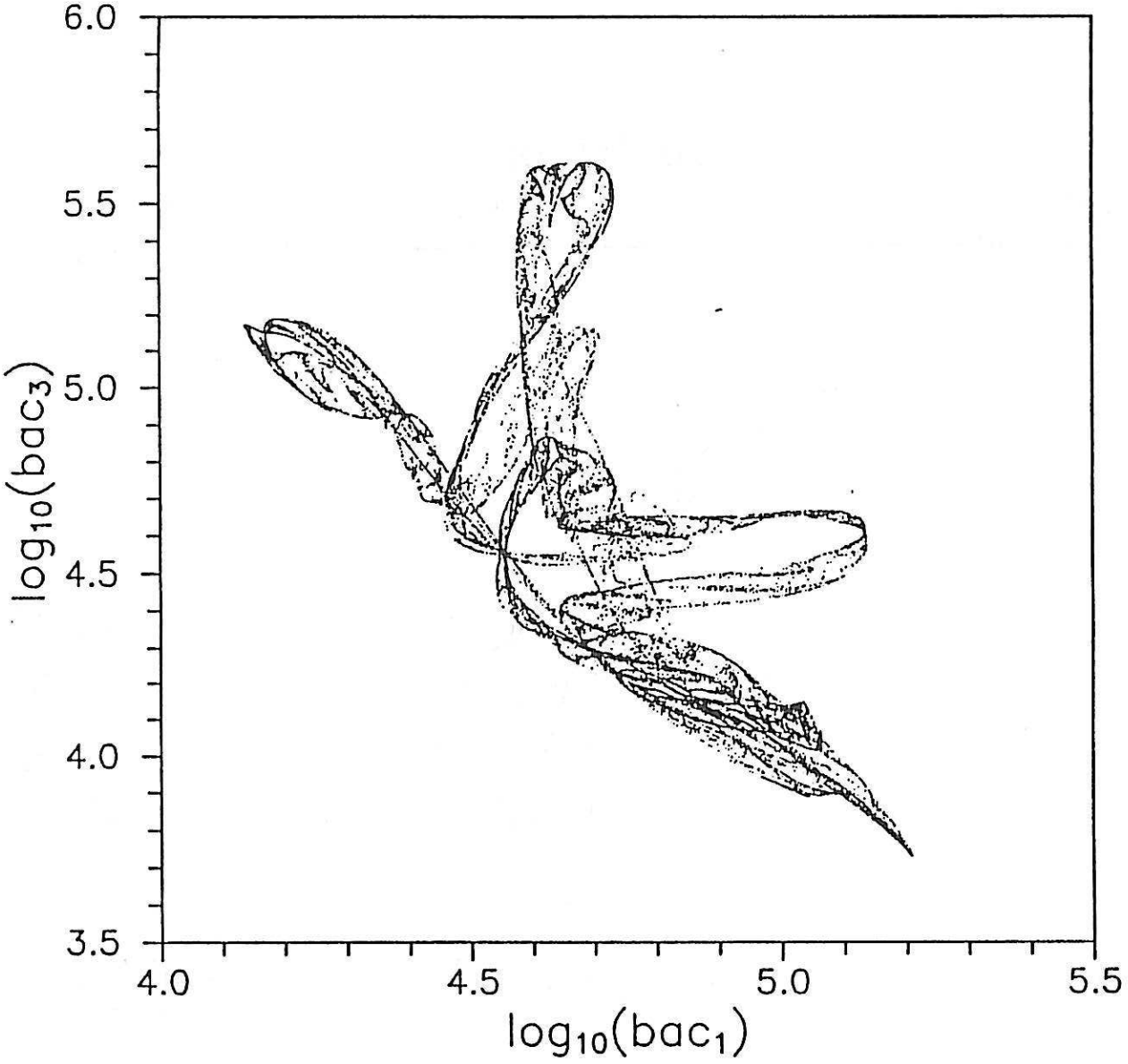

Baier et al.
Fig. 7

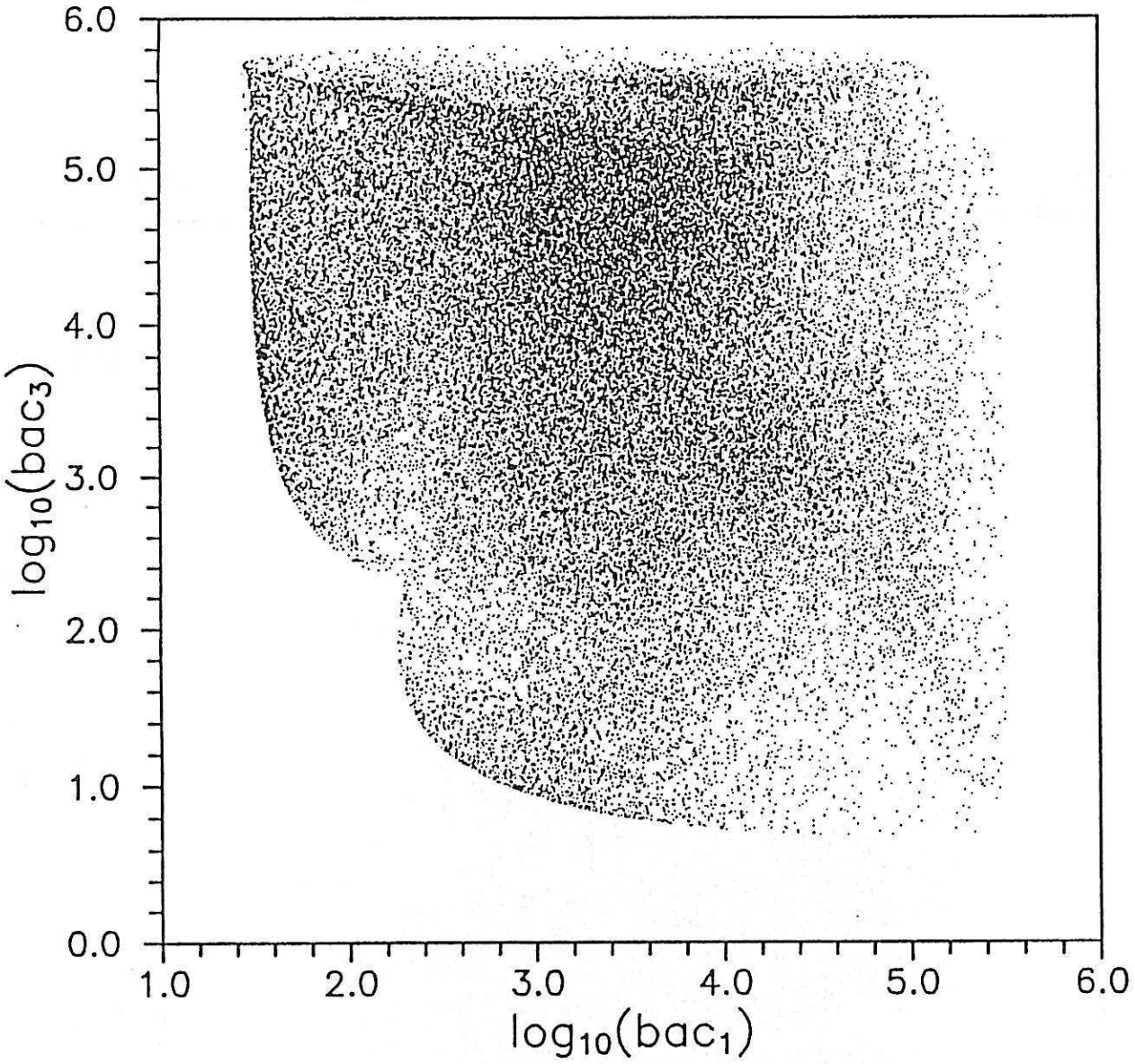

Baier et al.
Fig. 8

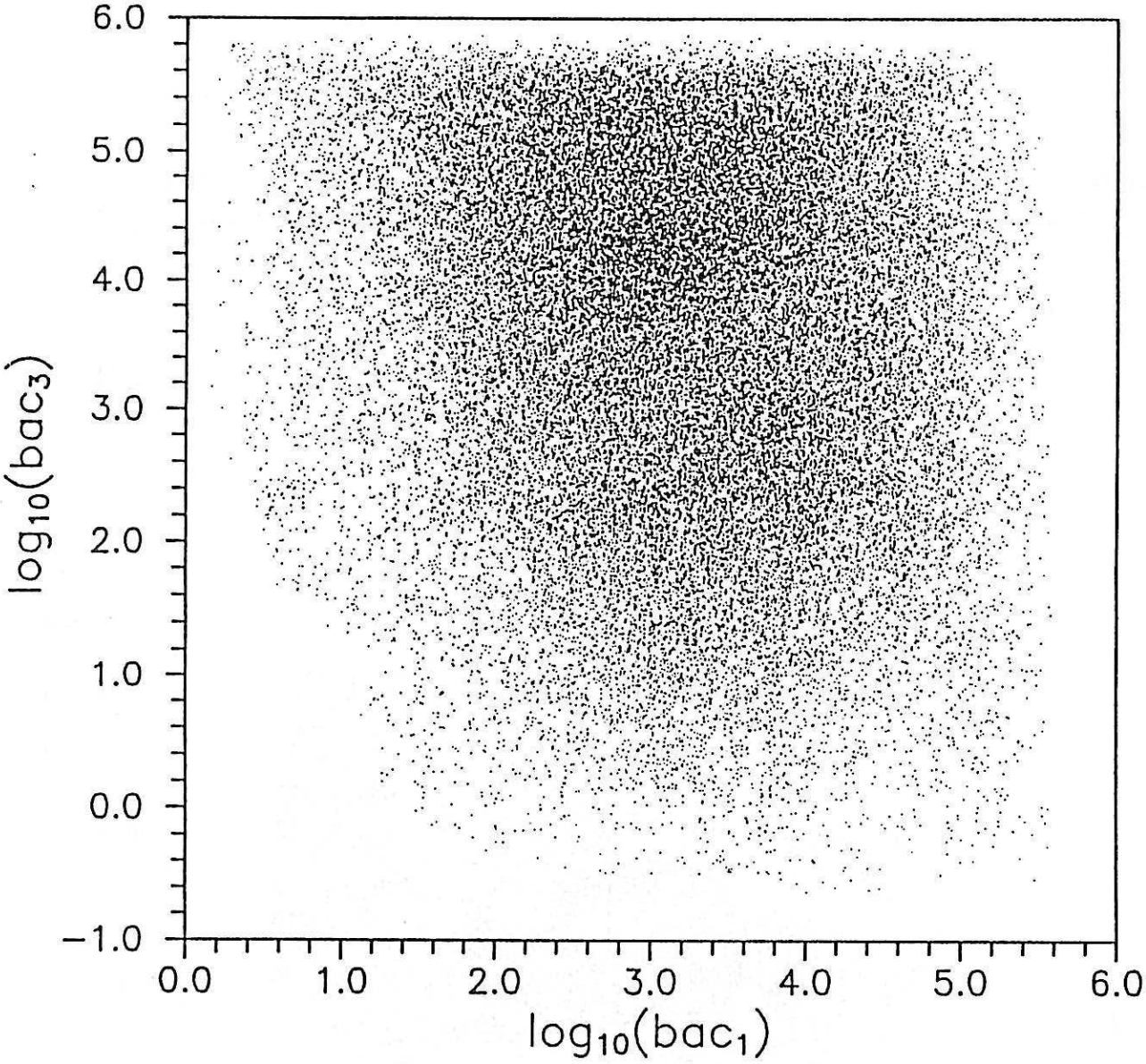

Baier et al.
Fig. 9